Electron Scattering by H_2 with and without Vibrational Excitation. III. Experimental and Theoretical Study of Inelastic Scattering

S. TRAJMAR,*,† D. G. TRUHLAR,† J. K. RICE,‡ AND A. KUPPERMANN†
California Institute of Technology, Pasadena, California 91103

(Received 17 November 1969)

The ratios of the differential cross sections (DCS's) for excitation of the first, second, and third vibrational states of H_2 in its ground electronic state to the elastic DCS have been measured as a function of scattering angle in the 10°–80° range and impact energy in the 7–81.6-eV range. From these ratios the DCS's corresponding to transitions from the ground to the first two vibrationally excited levels (fundamental and first overtone bands) were obtained by utilizing the elastic cross sections determined in the previous paper (II). In addition, the DCS for excitation of the second overtone band was determined for an impact energy of 10 eV. By angular extrapolation and integration of the DCS's the integral cross sections for the vibrational excitations were also determined. In addition, all these cross sections have been calculated using a quantum-mechanical method based on potential scattering in a plane wave scattering approximation which is described in Part I of this series. The present experimental and theoretical cross sections and previous measurements and calculations are compared. The calculated DCS ratios and the DCS's themselves for the fundamental excitation are in good agreement with experiment at 7 and 10 eV; however, at higher energies the calculated DCS's are generally larger than the experimental ones, at some angles by as much as a factor of 10. The calculated ratio of the DCS for the fundamental excitation to the elastic DCS shows a minimum as a function of angle, in qualitative agreement with the experimental results in the 13.6–81.6-eV energy range. The experimental DCS's for vibrational excitation also show a deep minimum. For excitation of the first overtone vibration, the experimental ratios are an order of magnitude larger than the calculated ones at low energy but in better agreement for the magnitude at higher energy. This discrepancy at low energies is explained in terms of resonance scattering. Our experiments are in good agreement with those of others in the few (low energy) cases where comparison is possible.

I. INTRODUCTION

Diffusion[1] and swarm[2,3] experiments carried out since the early 1930's have indicated the importance of vibrational excitation of molecular gases by low-energy electrons. However, the actual observation of discrete vibrational transitions and the detailed study of this phenomenon have become possible only recently with the advances of electron beam techniques.

Vibrational excitation of H_2 by low-energy electrons (below 10 eV) has been observed and studied by Schulz,[4] Menendez and Holt,[5] and Ehrhardt *et al.*[6] The scattering cross section was observed to have a maximum between about 2 and 4 eV, and the energy dependence [6–8] and angle dependence [6,9–11] of the cross section have been explained by resonance models at these low energies. Vibrational excitation of H_2 by electrons in the 11–13-eV range has been studied experimentally by Menendez and Holt[5] and others[12]; this scattering could be explained as due to contributions from higher energy resonances superimposed on a potential scattering background. Vibrational excitation in H_2 is optically forbidden and has not been observed at very high energies (35 keV)[13] where the first Born approximation predicts that optical electric dipole selection rules are approximately valid.

Our investigation is concerned with low-energy scattering at 7 and 10 eV and with the intermediate energy range (from 10 to 100 eV). The vibrational excitation in the intermediate energy range is expected to be due to potential scattering, but there have been no previous experimental investigations of it in this range. The ratio of the intensity of electrons scattered after causing a transition to a specific vibrational level of the ground electronic state of H_2 to the intensity of electrons scattered without having caused either vibrational or electronic excitation has been measured for scattering angles $\theta=10°$–$80°$, for impact energies $E=7$–81.6 eV, and for final vibrational levels $v'=1$–3. From these measurements and from the elastic differential cross sections[14] the vibrational differential cross sections have been obtained. By extrapolating the differential cross sections (DCS's) to 0° and 180°, the integral vibrational excitation cross sections were determined. The experiments do not resolve the rotational structure of the energy-loss processes.

We have also calculated the vibrational excitation cross sections by the quantum-mechanical method described in Paper I.[15] Our experimental and theoretical values are compared with the measurements of Ramien[1] ($E=3.5$ to 7.2 eV), Schulz[4] ($E=3$ to 8 eV), and Ehrhardt *et al.*[6] ($E=1$ to 10 eV), and with the calculational methods (low energy) of Breig and Lin[16] and Takayanagi.[17]

II. EXPERIMENTAL METHODS AND DATA HANDLING

Measurement of scattered signal intensities corresponding to vibrational excitation in H_2 requires a moderately high energy-loss resolution (about 0.1 eV or better) and a very sensitive detector. The first vibrational energy-loss feature is separated by only 0.52 eV from the elastic peak in the energy-loss spectrum, and the latter is in some cases 10^4 times stronger. The results presented here were obtained with the same

electron impact spectrometer used in II. The H_2 pressure was kept constant at about 10^{-3} torr as measured by an uncalibrated ion gauge. At this pressure the effect of double scattering is negligible for the type of DCS which occurs in the present case. While obtaining one spectrum, the electron impact energy (E) and scattering angle (θ) are fixed, and the energy-loss range from -0.2 to $+1.6$ eV is scanned. The sweep is repeated many times and the scattered intensities from each sweep are accumulated to form the final energy-loss spectrum. On the average about 10 h of multichannel scaling were necessary at each θ and E to build up an acceptable signal-to-noise ratio in the vibrational excitation part of the spectrum. A typical energy-loss spectrum is shown on Fig. 1. Study of the angular and energy dependence of the cross sections requires the collection of many spectra over a period of months. It cannot be expected that the instrumental conditions remain unchanged during these long data-collecting periods. In order to minimize the errors introduced by the changing instrumental conditions, the following experimental procedure was used:

(1) Each spectrum is a superposition of many repetitive energy-loss scans, where each scan has a duration of about 10 min. (Since the instrument is very stable for a few hours, the different parts of the spectrum are produced under identical conditions.)

(2) From each spectrum the ratios $R_{v'}=I_{v'}/I_0$ are measured for $v'=1$, 2, and 3, where $I_{v'}$ is the scattered intensity corresponding to excitation of the v' vibrational state and I_0 is the elastic scattering intensity. These ratios are the quantities that are least subject to experimental errors and are directly comparable at all angles.

(3) The elastic DCS's determined separately (Paper II) are then utilized to obtain the vibrational DCS's. The measurement of the elastic angular distribution[14] takes only about 3 h, during which the change in the experimental conditions can be made negligible.

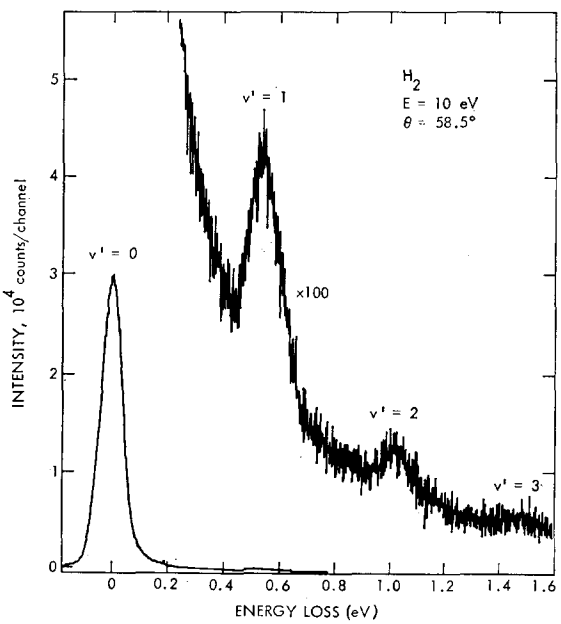

FIG. 1. Energy-loss spectrum of H_2 at $E=10$ eV and $\theta=58.5°$ (before smoothing). The spectrum is a superposition of 58 scans with 1 sec dwell time (time spent in one channel during each scan accumulating the scattered signal intensity) and 1.75-meV increments between adjacent channels.

As Fig. 1 shows, there is some contribution from the tail of the elastic peak to the vibrational intensities. This tail contribution, however, is a smoothly varying function of energy loss and is interpolated and subtracted from the composite signal. A practically complete resolution of the elastic scattering and vibrational excitation features would have been possible; this, however, would have appreciably increased the time required for the experiments. (The spectrometer is capable of about 0.030-eV resolution and can measure a signal that corresponds to one electron in every 20 sec.)

The spectrum accumulated in the detector memory was smoothed by averaging over three neighboring channels, and the intensity ratios $R_{v'}$ were calculated from the peak heights of the energy-loss features after subtraction of the background. Using the peak heights as a measure of intensity is acceptable since it was found that the line shape was independent of scattering angle. It was also experimentally established that the instrument efficiency was independent of energy-loss over the spectral range of interest here. [The gun, the energy selector, and entrance optics to the scattering chamber were tuned to generate the required electron beam and the second half of the apparatus was tuned to get the optimum elastic peak (maximum intensity at the required resolution) at 40°. With these settings, energy loss features about 6–8 eV away from the elastic peak were recorded at several lower and higher scattering angles, and then an attempt was made to reoptimize the second half of the instrument to give maximum signal for the inelastic features at the same resolution. In all cases it was found that no improvement was possible and that the optimum tuning conditions for the elastic feature were also the optimum conditions for the inelastic ones. This was not true for the inelastic features about 15–20 eV from the elastic peak.] Since the factors relating the peak intensities to their respective DCS's are the same for every energy-loss feature in any one spectrum, $R_{v'}=\mathrm{DCS}_{0v'}/\mathrm{DCS}_{00}$, where we denote the DCS for excitation of the v' vibrational state by $\mathrm{DCS}_{0v'}$ and the elastic DCS by DCS_{00}. Multiplication of $R_{v'}$ by the elastic DCS, which was determined previously (Paper II), gives the DCS for vibrational excitation in the 10°–80° angular range at each of seven individual impact energies. The incident energy scale was not calibrated and hence E can be in error by about ± 1 eV due to contact potentials. An angular extrapola-

tion and integration procedure similar to the one described in the previous paper (II) for the elastic scattering was applied to the $DCS_{0v'}$ to obtain the integrated vibrational excitation cross sections $Q_{0v'}$. Type 1 extrapolation[14] was used to calculate $Q_{0v'}$ for Table III of Paper II and for this paper. The error bars shown on the figures are typical values obtained by summing up all the estimated errors in the experimental and calibration procedures. Their values are approximately 10% for R_1, 20% for R_2, 30% for R_3, 45% for the DCS_{01}, 55% for the DCS_{02}, and 65% for the DCS_{03}.

III. CALCULATION METHODS

A calculation procedure using plane wave scattering wavefunctions, accurate unperturbed molecular vibrational wavefunctions, and model potentials based on quantum-mechanical considerations of the electronic charge distributions has been described in I.[15] This procedure represents an improvement over earlier less complete methods used by Carson,[18] Breig and Lin,[16] and others (see I for references). One method we use is to calculate in first-order perturbation theory the transition probability between unperturbed initial and final vibrational states, i.e., the Born approximation (BXP, where B stands for Born approximation and XP means without polarization). In addition, we sometimes make corrections to account for exchange effects; this gives the prior Born–Ochkur–Rudge approximation (BORXP, where BOR stands for Born–Ochkur–Rudge approximation). For accurate results, however, this method might have to be carried to at least second order in the scattering to include the distortion of the scattering electron wavefunction and/or to include the polarization of the electronic wavefunction of the bound electrons of H_2. In I, we describe a method of including polarization by adding to the static perturbation potential an effective (nonadiabatic) polarization potential based on variational calculations.[19] This is a common technique and it corresponds to a partial summation of the electronic polarization terms in the perturbation series. The results are the polarized Born approximation (B/P, where /P means plus polarization) and, when we include exchange effects, the polarized BOR approximation (BOR/P). Because the conditions for validity of the Ochkur–Rudge method of including exchange are not known, we generally present the results of both calculations. These methods neglect back coupling, the direct effect of distortion (which was considered by Takayanagi[17]), most of the effect of distortion on the exchange correction, and some other higher-order effects which might be important. The present calculations also do not include resonance effects. To test these methods, they were applied to calculate the elastic scattering cross sections for H_2 and shown in II to give good agreement with the experimental integral and differential elastic cross sections at and above 10 eV when the model potential (data set 1) which is considered theoretically most justified (see Paper I) is used in the calculation. Thus, in the present article we will continue to use this model. Then the effective interaction potential for direct scattering is[15]

$$V(\mathbf{r},\mathbf{R}) = V_0^C(r,R) - [\alpha(R)/2r^4]g_0^{D5}(r) + \{V_2^C(r,R) - [Q(R)/2r^3]f^{B'}(r) - [\alpha'(R)/2r^4]g_2^{D5}(r)\}P_2(\hat{r}\cdot\hat{R}), \quad (1)$$

$$g_L^{D5}(r) = 1 - \exp(-r^5/a_L^5), \qquad L=0,\,2, \quad (2)$$

$$f^{B'}(r) = 1, \qquad r > a_Q$$
$$= (r/a_Q)^3, \qquad f \le a_Q, \quad (3)$$

where $\mathbf{r}$ is the scattering electron coordinate, $\mathbf{R}$ is the intermolecular coordinate, V_0^C and V_2^C are terms in the Carson potential, α and α' are the spherical and asymmetric components, respectively, of the molecular electric dipole polarizability, Q is the molecular electric quadruple moment, g_L^{D5} and $f^{B'}$ are cutoff functions, and a_0, a_2, and a_Q are parameters. Scattering off the five interactions in Eq. (1) will be denoted S_0, P_0^{D5}, S_2, $Q^{B'}$, and P_2^{D5}, respectively. We will use data set 1 (DS1) except where explicitly stated otherwise.

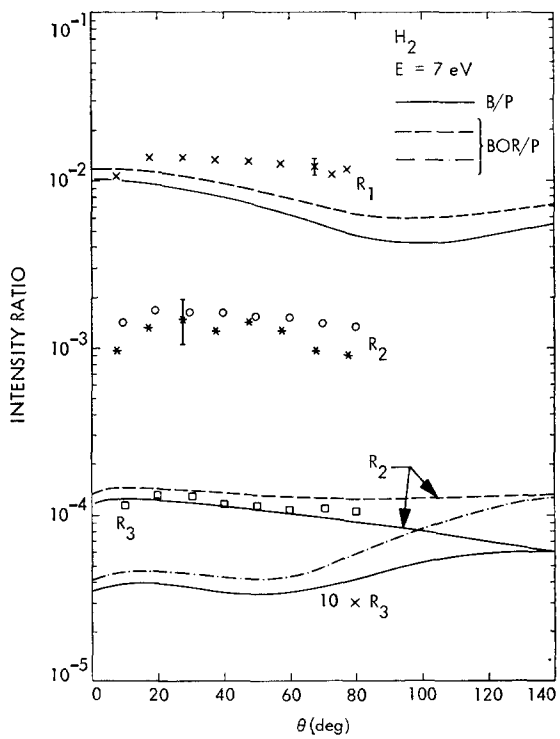

FIG. 2. The ratios $R_{v'}$ of the vibrational excitation to elastic scattering intensities as a function of scattering angle at $E=7$ eV. The indices 1, 2, and 3 on $R_{v'}$ refer to final vibrational quantum number $v'=1$, 2, and 3, respectively. The symbols × and * are our measured values for R_1 and R_2, respectively, and the symbols ○ and □ show the values obtained for R_2 and R_3, respectively, by using the data of Ehrhardt *et al.*[6] and the procedure described in Sec. IV.A of the text. The curves are the results of the present calculation.

DS1 implies $a_0=2.1$ a.u., $a_2=1.8$ a.u., and $a_Q=2.0$ a.u. Sometimes calculations using these three parameters of DS1 but using

$$g_L^A(r)=r^4(r^2+a_L^2)^{-2} \tag{4}$$

or

$$g_L^B(r)=1, \qquad r>a_L$$
$$=r^4a_L^{-4}, \qquad r\leq a_L. \tag{5}$$

instead of g_L^{DS} in Eq. (1) are also presented; they are labeled (A) or (B). Finally, a calculation using Eqs. (1)–(3) with the parameters $a_0=a_2=a_Q=1.7a_0$ is also shown and labeled DS 1.7.

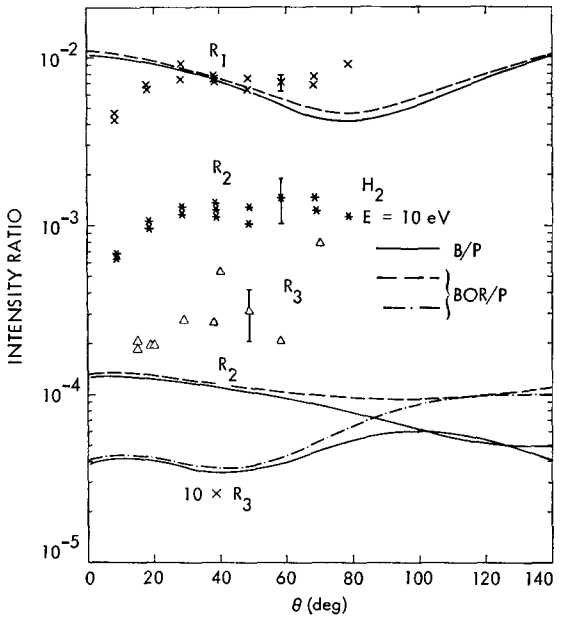

FIG. 3. The ratios R_v' of the vibrational excitation to elastic scattering intensities as a function of scattering angle at $E=10$ eV. The symbols ×, *, and Δ are our measured values for R_1, R_2, and R_3, respectively. The curves are the results of the present calculation.

IV. RESULTS AND DISCUSSION

A. Angular Dependence of Intensity Ratios

The experimentally measured R_v's are not subject to uncertainties introduced by the effective path length correction, the normalization procedures, and changes in instrumental conditions which are slow with respect to the sweep time for one energy-loss scan. We pointed out in Sec. II that these ratios are equal to the corresponding cross section ratios. The experimental and calculated intensity ratios as a function of scattering angle are given in Figs. 2–10. On Figs. 4 and 7, several separate measurements of R_1 taken over periods of up to half a year are shown to demonstrate the reproducibility.

At scattering angles 10°–15° and below the direct beam contribution to the elastic scattering signal can

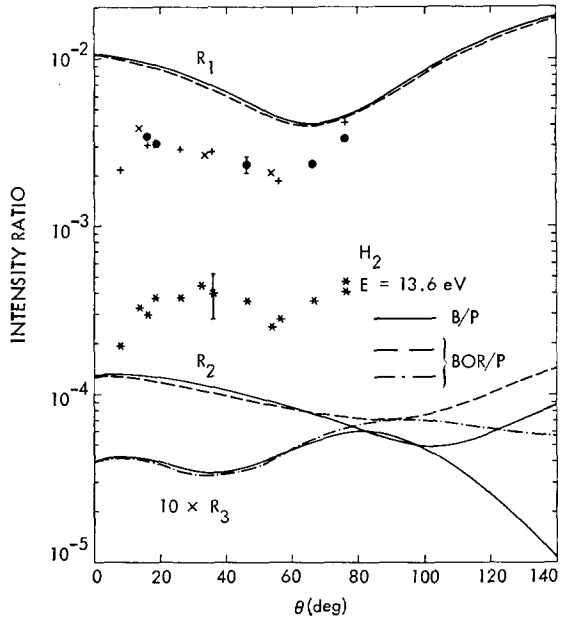

FIG. 4. Same as Fig. 3, except $E=13.6$ eV and the symbols +, ×, and ● represent three measurements of R_1 taken at different times. No experimental R_3 ratios are available.

be important[14]; therefore, the errors in the ratios and DCS's can be considerably greater at 10° than at larger angles.

Other experimental R_v's in this energy region with which our measurements can be compared are those which we can obtain from the measurements of Schulz[4]

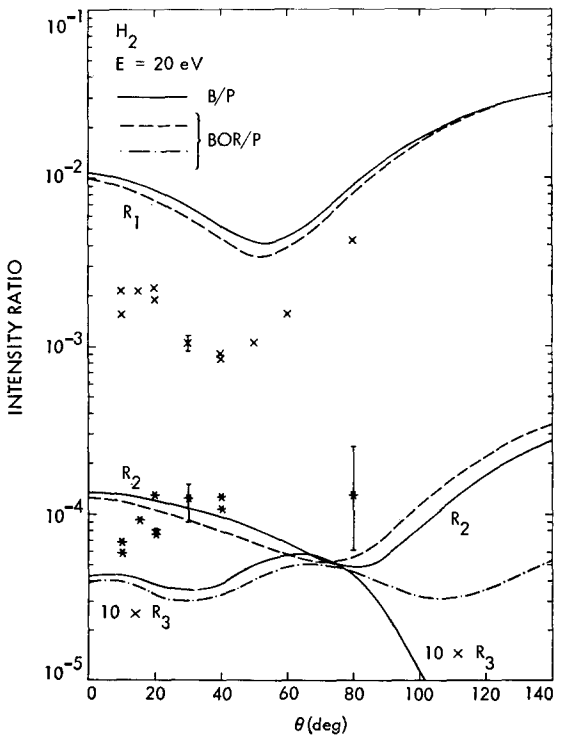

FIG. 5. Same as Fig. 3, except $E=20$ eV.

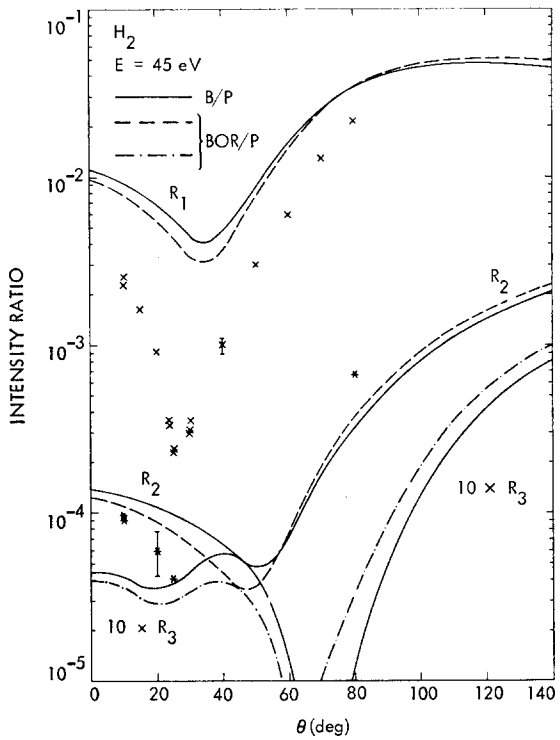

FIG. 6. Same as Fig. 3, except $E=45$ eV.

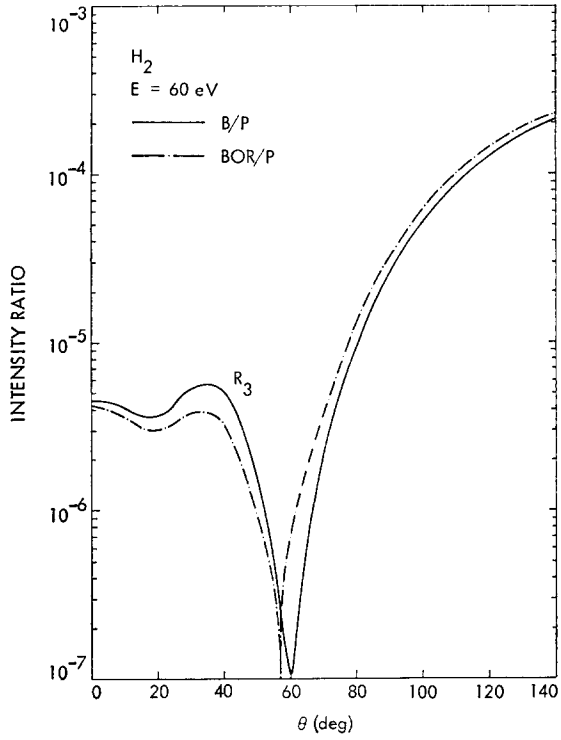

FIG. 8. The calculated values of R_3 as a function of scattering angle at $E=60$ eV.

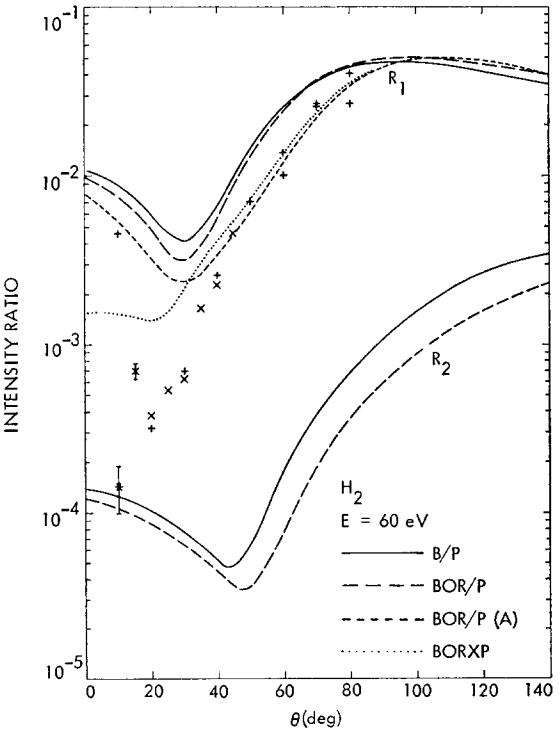

FIG. 7. The ratios $R_{v'}$ of the vibrational excitation to elastic scattering intensities as a function of scattering angle at $E=60$ eV. The symbols + and × are two separate measurements of R_1, and the symbol * is a measured R_2 value. The curves are the results of the present calculation. (See Sec. IV.A of the text for an explanation of the curves.)

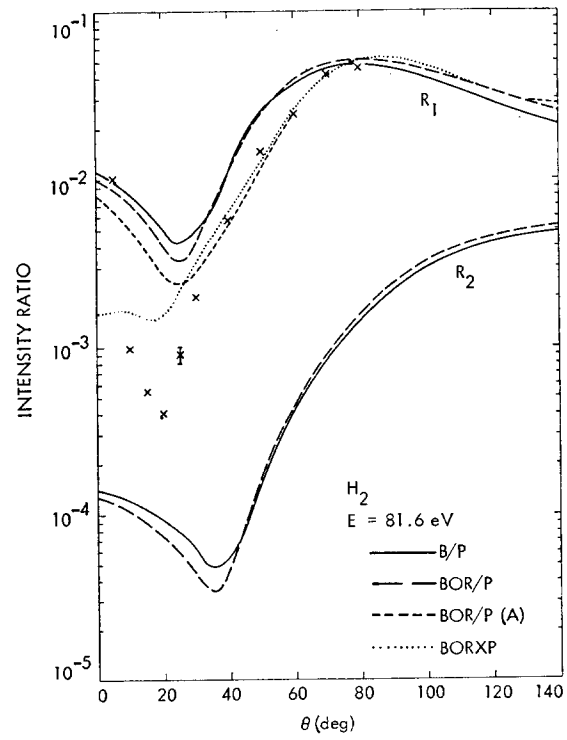

FIG. 9. The ratios $R_{v'}$ of the vibrational excitation to elastic scattering intensities as a function of scattering angle at $E=81.6$ eV. The symbols × are our measured values for R_1. The curves are the results of the present calculation. (See text for explanation of curves.)

and of Erhardt *et al.*[6] Schulz's data is considered in Sec. IV.C. Ehrhardt *et al.* give $Q_{0v'}$ for $v'=1$, 2, and 3 as a function of impact energy from about 1 to 10eV. They found that the shapes of the angular distributions for $20°\leq\theta\leq110°$ for the $v'=1$ and 2 (and presumably for the $v'=3$) channels were the same and were independent of impact energy from about 1 to 10 eV within their experimental errors (about 10%). Therefore, the ratios DCS_{02}/DCS_{01} and DCS_{03}/DCS_{01} should be independent of angle and equal to $Q_{01}/Q_{02}=8.3$ and $Q_{01}/Q_{03}=1.0\times10^2$. These ratios combined with our ratio R_1 at several angles yield the values representing their R_2 and R_3 in Fig. 2. The agreement with our experimental values for R_2 is good.

At $E=7$, 10, and 13.6 eV, the calculated R_1 curves agree fairly well with the measured ones both in magnitude and shape. As one goes to higher impact energies, the experimental ratio curves develop deep minima around 20°–40° scattering angles. At these energies the calculated curves are in poorer agreement as they do not reproduce the dips quantitatively. There is, however, still an order of magnitude agreement with experiment, and the experimentally observed shift of the minimum in the ratio curves to lower angles with increasing impact energy is properly predicted by the calculations. The BOR/P curves give somewhat better agreement with experiment than the B/P ones. The difference, however, is not always significant and becomes negligible at some energies. At low angles the term which has the largest effect on the calculated scattering cross section is the polarization potential, as expected from its long-range nature. This is shown on Figs. 5 and 7 and in Paper I.

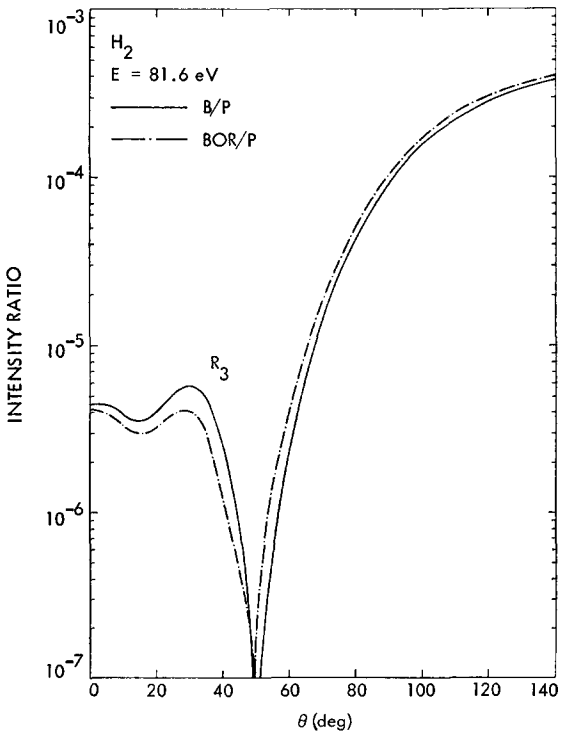

FIG. 10. The calculated values of R_3 as a function of scattering angle at $E=81.6$ eV.

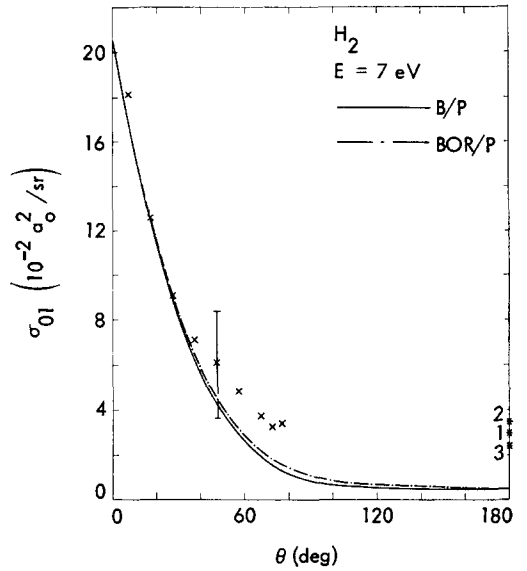

FIG. 11. Differential cross sections for the excitation of the fundamental vibration ($v'=1$) in H_2 by 7-eV electrons. The symbols × are our measured values and the curves are our calculated values. The asterisks at 180° show the values of the DCS predicted there by the three methods of extrapolation discussed in Sec. III of Paper II.

The calculated values for R_2 and R_3 are about a factor of 10 less than the experimental ones at 7 and 10 eV, but at higher energies the agreement for R_2 is much better. The discrepancies at 7 and 10 eV probably are due to inaccuracies in the vibrational excitation DCS calculation and will be discussed in Secs. IV.B and IV.E. The calculated R_3 curves are also shown above 10 eV, although at the present time no experimental data are available for comparison.

Figures 7 and 9 show the R_1 values calculated by the BOR model with form A for the polarization potential[15] [curve BOR/P(A)] and when polarization is neglected (Curve BORXP). (See Paper I for further discussion of these methods.) These curves show that the polarization potential is necessary for producing the deep dip in the R_1 ratio but that the exact form of the polarization potential for small electron–H_2 distances (r) is not crucial in determining the shape of the curve in the vicinity of the dip. This is true at all energies above 10 eV except that at energies of several hundred electron volts the dip appears prominently in the calculation even without polarization and the effect of including the polarization potential is to make it deeper.

B. Angular Dependence of the DCS

The vibrational excitation DCS's as a function of scattering angle are shown in Figs. 11–21. Calculations using the B/P and BOR/P approximations are shown.

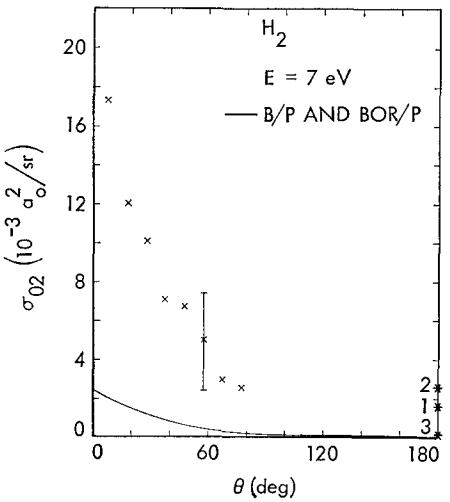

FIG. 12. Differential cross sections for the excitation of the first overtone vibration ($v'=2$) in H_2 by 7-eV electrons. The symbols × are our measured values, and the curve is from our calculations. The asterisks at 180° are explained in the caption of Fig. 11.

When only the former is indicated, the BOR/P curve would not deviate noticeably from the B/P one. The absolute values for the experimental measurements were obtained from the normalized elastic cross sections (Paper II) and from the experimentally determined $R_{v'}$ as described in Sec. II. On the right-hand side of each figure, the values of the DCS at the highest angle shown on that figure are given as obtained by the three different extrapolation methods described in II. Type 1 extrapolation has been used to calculate the integral cross sections.

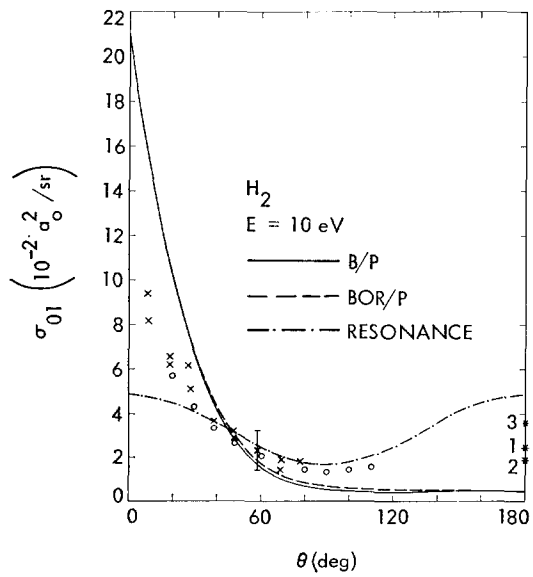

FIG. 13. Differential cross sections for the excitation of the fundamental vibration ($v'=1$) in H_2 by 10-eV electrons. The open circles and crosses are the measurements of Ehrhardt *et al.* (Ref. 6) and the present measurements, respectively. The curve labeled RESONANCE is proportional to $(1+2\cos^2\theta)$ and is normalized to experiment at 40°. The solid and the dashed curves are the results of the present calculation. The asterisks at 180° are explained in the caption of Fig. 11.

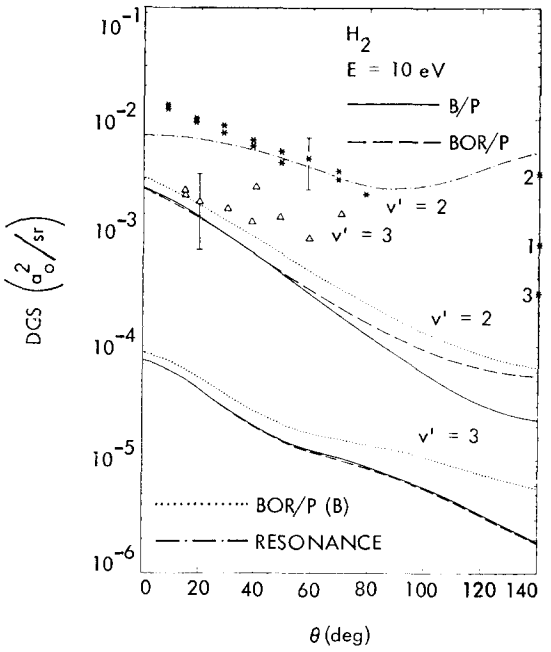

FIG. 14. Differential cross sections for the excitation of the first (*) and second (Δ) overtone vibrations in H_2 by 10-eV electrons. The resonance curve corresponds to a $(1+2\cos^2\theta)$ angular distribution and is normalized to experiment at 50°. The other curves are the results of the present calculation. (See text for explanation of the curves.)

Figure 13 also shows the angular distribution measured by Ehrhardt *et al.*[6] for the first vibrational excitation at 10 eV. Their cross section was given in arbitrary units and for purposes of display has been

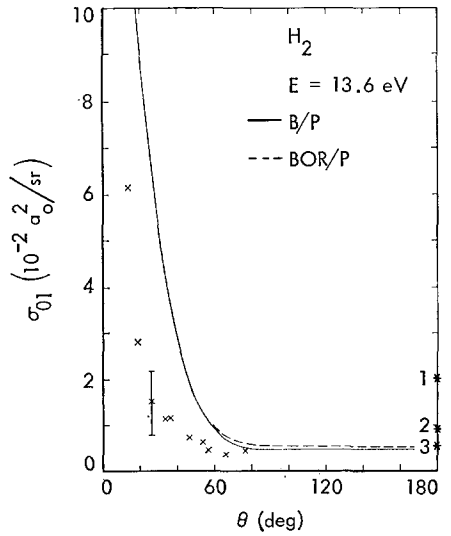

FIG. 15. Differential cross sections for the fundamental vibrational excitation in H_2 by 13.6-eV electrons. The ×'s are the present experiments, the curves are the present calculations, and the asterisks are explained in the caption of Fig. 11.

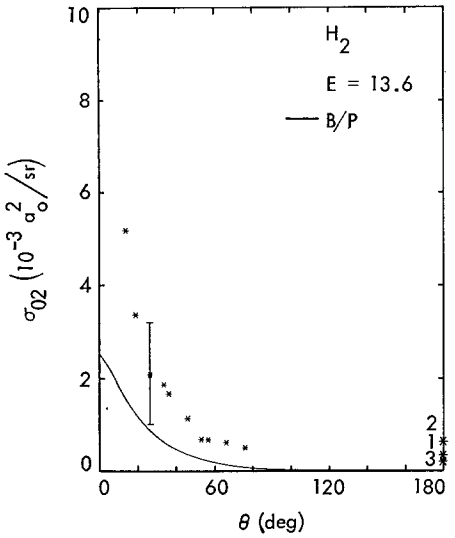

FIG. 16. Differential cross sections for the excitation of the first overtone vibration in H_2 by 13.6-eV electrons. The *'s below 90° are the present experiments, and the asterisks at 180° are explained in the caption of Fig. 11. The curve is the result of the present calculation.

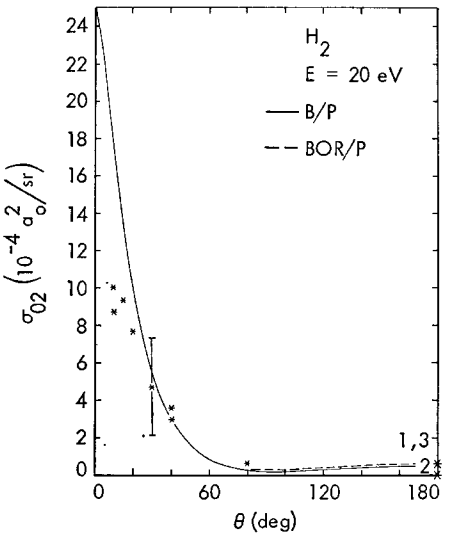

FIG. 18. Same as Fig. 16, except $E=20$ eV.

normalized to our experimental one at 60°. The two experimental angular distributions are in excellent agreement. The dash–dot curve on Fig. 13 is obtained from the expression $\mathrm{DCS}(\theta) \propto (1+2\cos^2\theta)$ by normalizing it to experiment at 40°. This type of angular behavior is predicted by resonance theories for scattering by means of a $^2\Sigma_u^+$ intermediate negative-ion state.[6,9,10] Although the predicted angular distribution of the resonance model is in good agreement with experiment above 40°, at the lowest angles there is a considerable disagreement. O'Malley and Taylor[9] suggested that the deviation could be due to scattering by higher partial waves, e.g., f waves. In our model the strong forward scattering is due to scattering in many higher partial waves by the polarization potential. The direct scattering model (B/P) curve gives just as good or better agreement with experiment as the resonance model and requires no empirical scale adjustment.

As noted in Sec. IV.A, Erhardt *et al.*[6] found that the shapes of the angular distributions for vibrational excitation of the $v'=1$ and 2 states were independent of energy from about 1 to 10 eV and were the same for both states. Our 7- and 10-eV measurements do not eliminate this as a possibility within the limits of

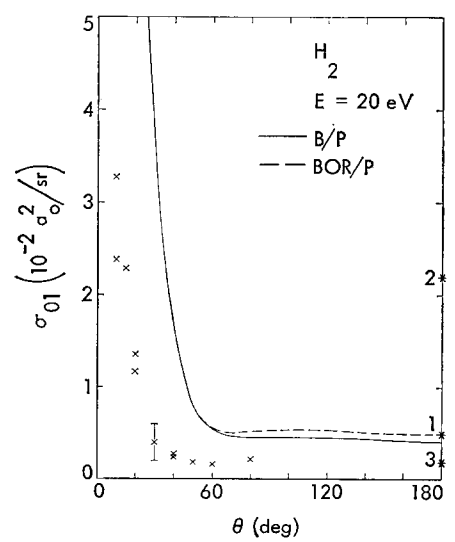

FIG. 17. Same as Fig. 15, except $E=20$ eV.

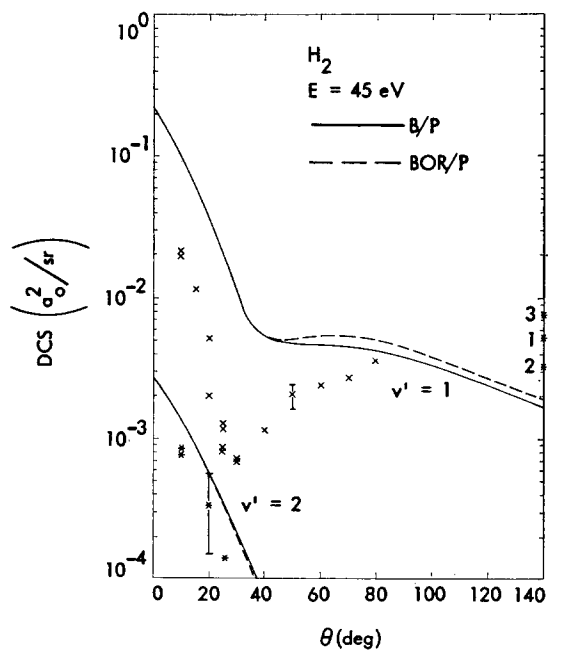

FIG. 19. Differential cross sections for the excitation of the fundamental (×) and first overtone (*) vibrations in H_2 by 45 eV electrons. The asterisks at 180° represent possible extrapolations of the $v'=1$ experiments. The curves are the results of the present calculation.

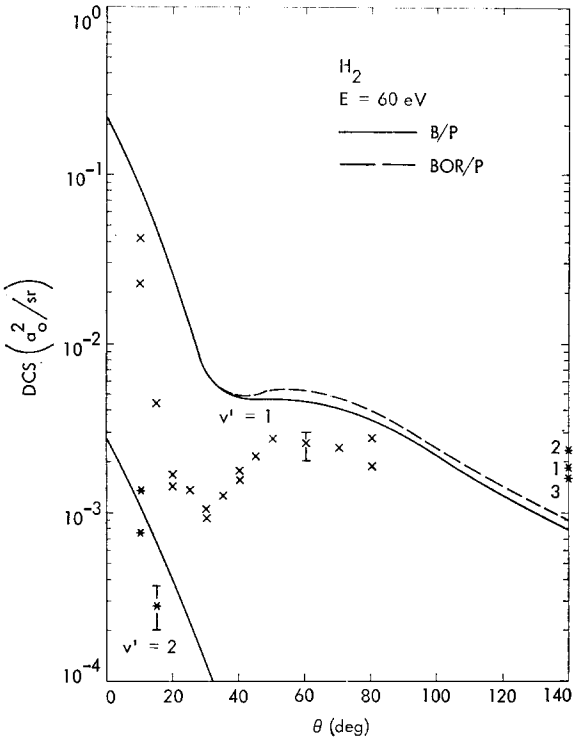

FIG. 20. Same as Fig. 19, except $E=60$ eV.

experimental errors. In fact, if the angular distribution of Erhardt *et al.* for $v'=1$ at $E=10$ eV and our four DCS's for $E=7$ and 10 eV and $v'=1$ and 2 are all normalized at 36°, a median DCS can be obtained and all the data points of these five DCS's in the 8°–80° range fall within 20% of it. Within the limits of our much larger 42% estimated error for the shape of DCS_{03}, even these points are consistent with the median DCS. Ehrhardt *et al.*[6] argued that the excitation cross section must be dominated by resonance scattering at all energies up to 10 eV since the shape of the angular distribution is practically independent of impact energy in that range. While it is true that pure resonance scattering would lead to a DCS whose shape is exactly the same over the whole width of the resonance, it is possible that the shape of the angular distribution due to potential scattering would also be fairly independent of impact energy over some energy range. Since we have shown in the previous paragraph that a potential scattering explanation of the $v'=1$ vibrational excitation is not precluded in the 7–10-eV energy range, this could be an example of inelastic scattering with an appreciable contribution from potential scattering which still exhibits a DCS whose shape does not change much with energy. Further support for such a possibility comes from the calculations for potential scattering in the B/P approximation shown in Table I. The shape of the DCS from 0° to 120° does not change much between 7 and 10 eV. Such a phenomenon could also occur in more accurate calculations. Another example is the excitation of the 2^1P state of helium by electrons with energies in the 34–55.5-eV range. The DCS's for this process have been determined in the $10°\leq\theta\leq70°$ region, and their shape changes only slightly more than experimental error in this nonresonance energy range.[20] These examples indicate that approximate energy-independence of the DCS shape is a necessary but not sufficient criterion for pure resonance scattering.

Above 10 eV the experimental DCS_{01} exhibits a gradual change in shape. A minimum and a maximum develop in the 10°–80° range, and they shift progressively to lower angles with increasing impact energies.

The B/P (or BOR/P) calculation is in good agreement with measurements at 7 and 10 eV for the excitation of the fundamental vibration. At higher energies, however, the agreement becomes poor, and the minimum found in the experimental angular distributions is not reproduced quantitatively by the calculations. (This is the source also for the disagreement in the experimental and calculated R_1 curves at the higher energies.) The polarized Born approximation evidently overestimates the potential scattering cross section for excitation of the first excited vibrational level of H_2.

For the excitation of the first overtone ($v'=2$) at 7 and 10 eV the calculated cross sections are about a

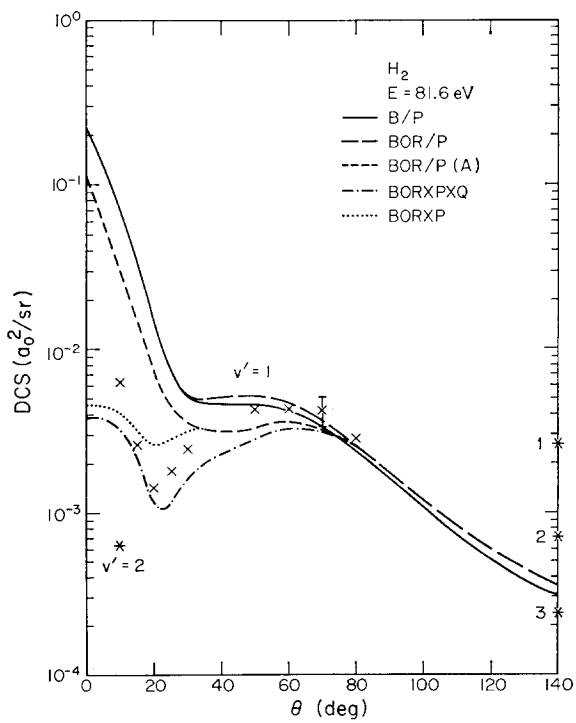

FIG. 21. Differential cross sections for the excitation of the fundamental and first overtone vibrations in H_2 by 81.6-eV electrons. The symbols are as in Fig. 19. The results of a BOR calculation without polarization and quadrupole interaction terms in the potential are also shown (BORXPXQ). The curves are the results of the present calculation. (See text for explanation of the other curves.)

TABLE I. Differential cross sections (a_0^2/sr) for vibrational excitation due to potential scattering (calculated in the polarized Born approximation) at low energies.

v'	1	1	1	1	1	1	1	1	1
Data set[a]	1	1	1	1	1	1	L	L	L
					E (eV)				
θ (deg)	1.8	3.4	5	7	10	25	5	7	10
0	0.164	0.187	0.195	0.201	0.206	0.214	0.169	0.174	0.178
12	0.151	0.157	0.154	0.147	0.138	0.106	0.131	0.125	0.117
24	0.129	0.123	0.112	0.100	0.086	0.045	0.093	0.083	0.071
36	0.109	0.095	0.080	0.066	0.051	0.016	0.066	0.054	0.041
48	0.092	0.072	0.056	0.042	0.028	0.007	0.046	0.034	0.023
60	0.077	0.055	0.039	0.026	0.015	0.005	0.031	0.021	0.012
75	0.063	0.039	0.024	0.014	0.008	0.005	0.020	0.012	0.007
90	0.051	0.028	0.015	0.009	0.005	0.005	0.013	0.007	0.005
105	0.042	0.020	0.010	0.006	0.005	0.004	0.009	0.006	0.004
120	0.035	0.015	0.008	0.005	0.005	0.004	0.007	0.005	0.004
v'	2	2	2	2	2	2	3	3	3
Factor[b]	10^2	10^2	10^2	10^2	10^2	10^2	10^4	10^4	10^1
Data set	1	1	1	1	1	1	1	1	1
					E (eV)				
θ (deg)	1.8	3.4	5	7	10	25	3.4	7	10
0	0.145	0.200	0.222	0.234	0.245	0.262	0.552	0.710	0.759
12	0.140	0.181	0.188	0.187	0.180	0.145	0.517	0.595	0.586
24	0.128	0.150	0.144	0.133	0.118	0.068	0.440	0.425	0.375
36	0.115	0.120	0.108	0.092	0.074	0.030	0.358	0.288	0.213
48	0.101	0.096	0.080	0.063	0.046	0.012	0.284	0.198	0.155
60	0.089	0.076	0.059	0.043	0.028	0.005	0.226	0.147	0.118
75	0.076	0.057	0.041	0.027	0.015	0.002	0.174	0.114	0.093
90	0.065	0.044	0.029	0.017	0.008	0.002	0.141	0.095	0.071
105	0.057	0.035	0.021	0.011	0.005	0.003	0.120	0.081	0.050
120	0.050	0.028	0.016	0.008	0.003	0.004	0.107	0.067	0.033

[a] See Paper I.
[b] The factor, if given, is the number by which the cross sections have been multiplied.

factor of 10 smaller than the experimental ones. At 13.6 eV this factor is only about 2, and from 20 eV on the calculated and measured cross sections are in good agreement. This discrepancy at low energy is also present in the R_2-ratio-versus-scattering-angle curves discussed previously and seems to be due to resonance contributions. Although the peak of the resonance is in the 2–4-eV impact energy range and its half-width is about 3 eV,[6] the resonance tail contribution is apparently still the dominant part of the overtone excitation cross section up to over 10 eV impact energy. Thus the resonance is more important for σ_{02} than for σ_{01}. This is discussed further in Sec. IV.E. Figure 14 compares the DCS_{02} with the $1+2\cos^2\theta$ angular distribution predicted by the resonance model (see above). The agreement at lower angles is poor.

There is only a limited amount of experimental data on the second overtone excitation. At 10 eV we find experimentally that the ratio DCS_{02}/DCS_{03} is about 4 and that DCS_{03} looks somewhat more isotropic than either DCS_{02} or DCS_{01}. This qualitative behavior is also shown by the calculation, but the calculated cross section is about 10 times smaller. The quantitative disagreement is again probably due to resonance contributions.

Figure 21 shows the results of calculations at 81.6 eV with form A of the polarization potential [BOR/P(A)], with a potential where the polarization terms were omitted (BORXP), and with a potential where both polarization and quadrupole terms were neglected (BORXPXQ). At this high impact energy it is hard to decide which of the calculations gives better agreement with experiment. This also has been found in some cases for the elastic scattering (see Papers I and II) and is attributed to the partial failing of the static polarizability model at high impact energies. More accurate experimental differential cross sections for $\theta \leq 10°$ would provide a more critical test of this point.

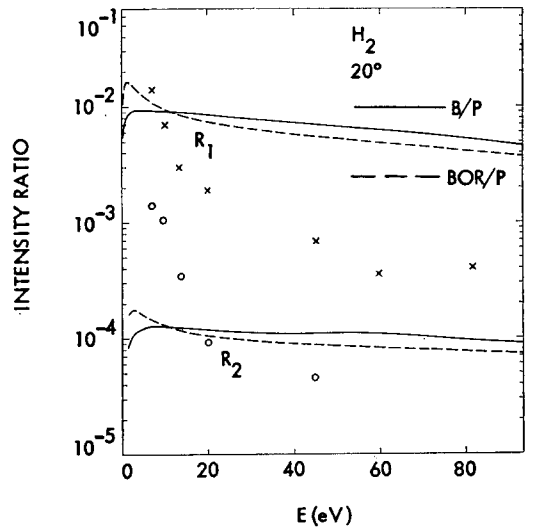

FIG. 22. Intensity ratios as a function of impact energy at 20° scattering angle. Crosses and open circles are the experimental R_1 and R_2 values, respectively; the curves are the results of our calculations. (See text for explanation of the curves.)

C. Energy Dependence of the Intensity Ratios

It is of some interest to look at the energy dependence of the intensity ratios in a more explicit form. Figures 22–27 show the ratios R_1 and R_2 at 20°, 30°, 40°, 60°, 70°, and 80° scattering angles as a function of impact energy. The experimental R_1 curves have a minimum as a function of impact energy. This minimum becomes more pronounced and shifts to lower impact energies as the scattering angle increases. The agreement between the calculations and experiments is poor at low angles but reasonably good above 40°. The minimum and its shift to lower energies with increasing angle is properly predicted by the calculations. The R_2 curves behave similarly to the R_1 curves, but for the former the experimental data extend only to 40 eV at 20° and 30° and only to 20 eV at higher angles.

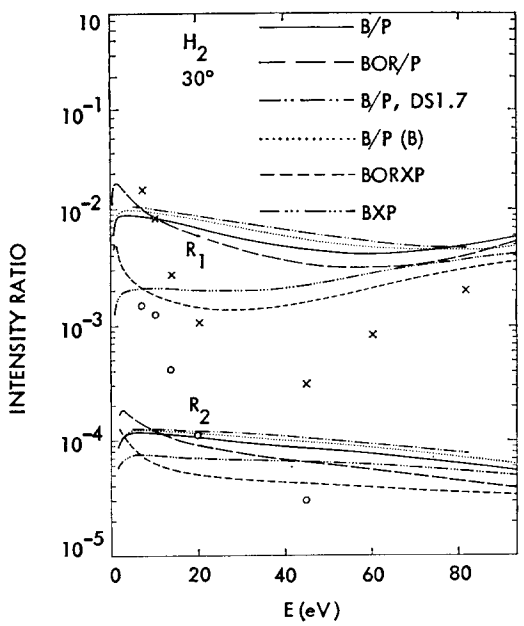

FIG. 23. Same as Fig. 22, except $\theta=30°$.

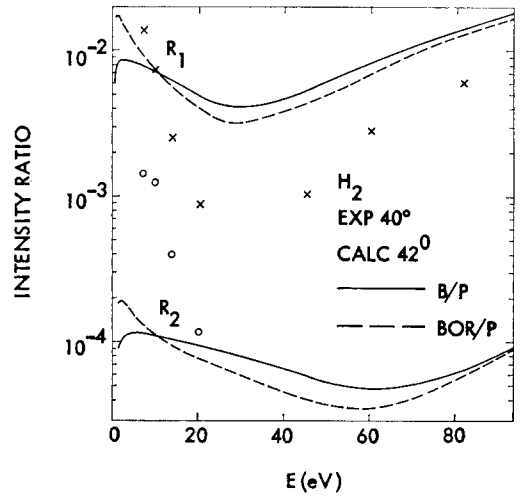

FIG. 24. Same as Fig. 22, except $\theta=40°$.

Figure 26 shows the intensity ratios R_1 measured by Schulz[4] at 72° scattering angle. He gave the integral cross section for the fundamental vibrational excitation as a function of impact energy (Fig. 11 of Ref. 4). He obtained these cross sections from his measured ratios of vibrational excitation to elastic scattering intensities at 72° and from the total electron–hydrogen-molecule scattering cross sections of Ramsauer and Kollath[21]

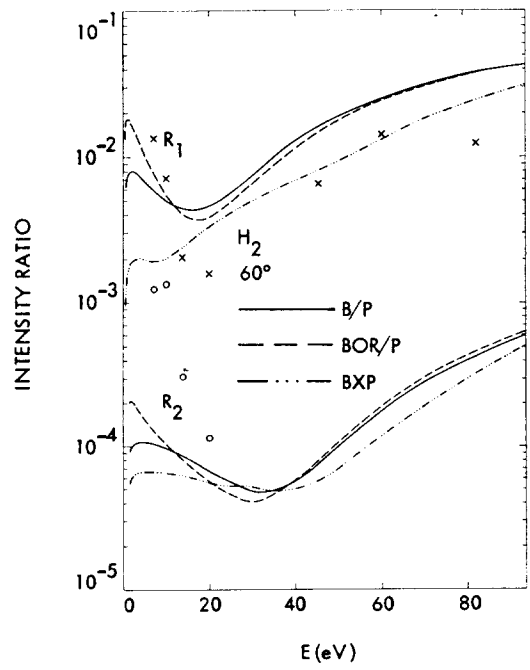

FIG. 25. Same as Fig. 22, except $\theta=60°$.

by assuming the angular dependences of the elastic and inelastic cross sections to be the same. Since DCS_{00} and DCS_{01} are now known not to have exactly the same shape (or else our ratios R_1 would be independent of angle), the most meaningful results from Schulz's measurements are the ratios R_1 at 72°. We have back-calculated his intensity ratios, and they are shown in Fig. 26. The agreement with our measurements is excellent. This is a most significant check on the measurements since these ratios were obtained directly from two different instruments and since, as mentioned previously, the ratios are the quantities least subject to experimental errors.

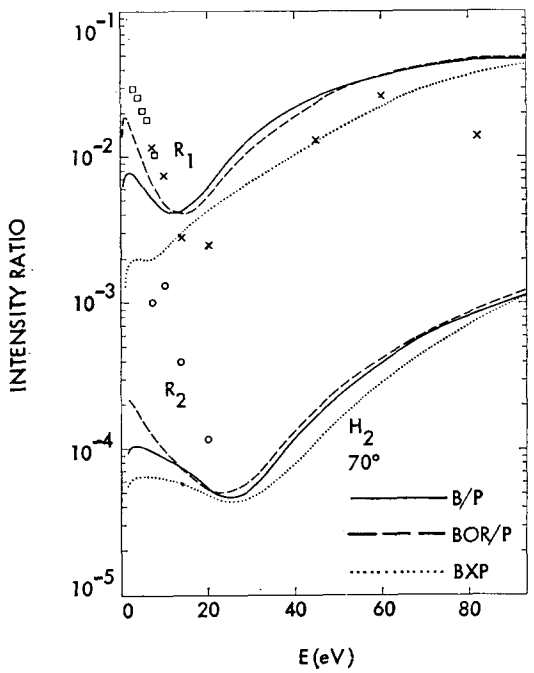

FIG. 26. Same as Fig. 22, except $\theta=70°$. The R_1 values measured by Schulz at 72° are also shown as boxes.

At $E=3.4$ eV and $\theta=72°$, Schulz also observed excitation of the $v'=2$ vibrational level.[4] From Fig. 11 of his paper one gets $[DCS_{02}(72°)/DCS_{01}(72°)]=Q_{01}/Q_{02}=0.20$, while the value of the same ratio is 0.074 from Fig. 5 of Ref. 6. For a wide range of choices of scattering potential (and with and without exchange and/or polarization) we calculate values of this quantity in the range 0.013–0.040 with 0.0145 for the theoretically most justifiable potential including polarization. This discrepancy indicates either that potential scattering contributions are proportionately much less important for $v'=2$ than for $v'=1$ even at $E=3.4$ eV (which is very near the nominal "resonance energy") and/or that our first-order calculation is very bad, even for the nonresonance part of the cross section at this low energy. From the discussions in Secs. IV.B and IV.E, it appears that the former alternative may be correct.

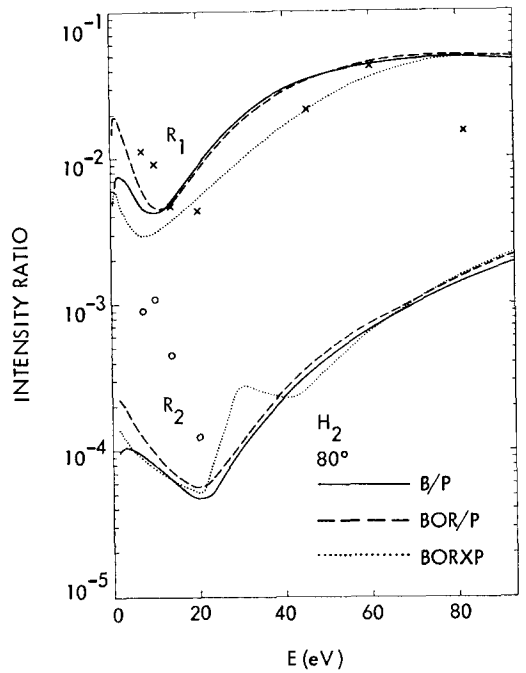

FIG. 27. Same as Fig. 22, except $\theta=80°$.

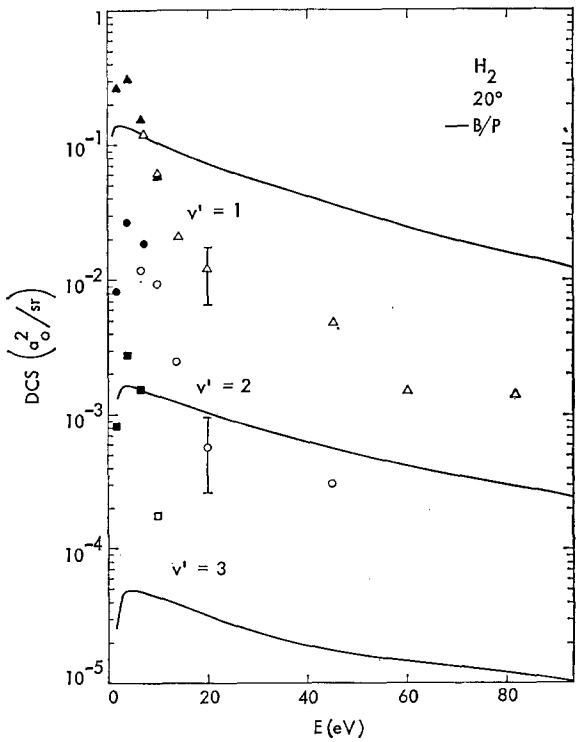

FIG. 28. The energy dependence of the 120° differential cross sections for the fundamental, first, and second overtone excitation in H_2 (Δ, ○, and □, respectively). The low-energy values indicated by filled-in symbols represent the measurements of Ehrhardt *et al.* The curves are the results of the present calculation.

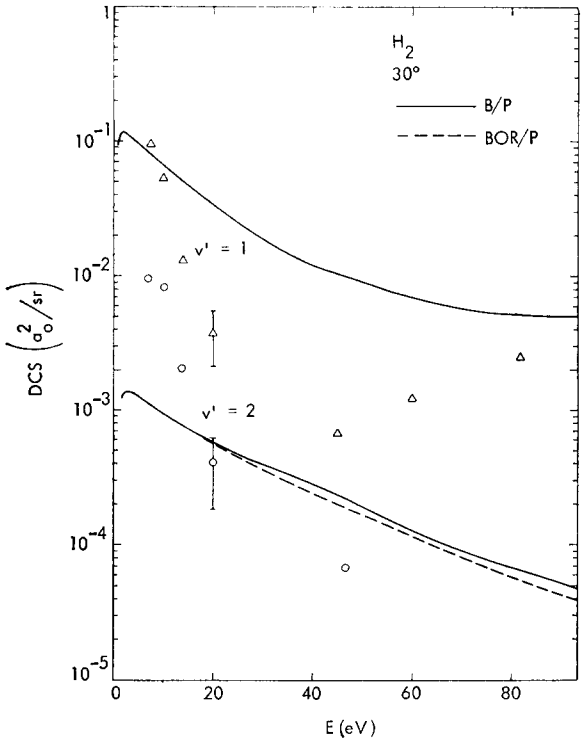

FIG. 29. The energy dependence of the DCS at 30° for the excitation of the fundamental (△) and first overtone (○) vibrations. The symbols are the present experiments and the curves are the results of the present calculation (two typical error bars are shown).

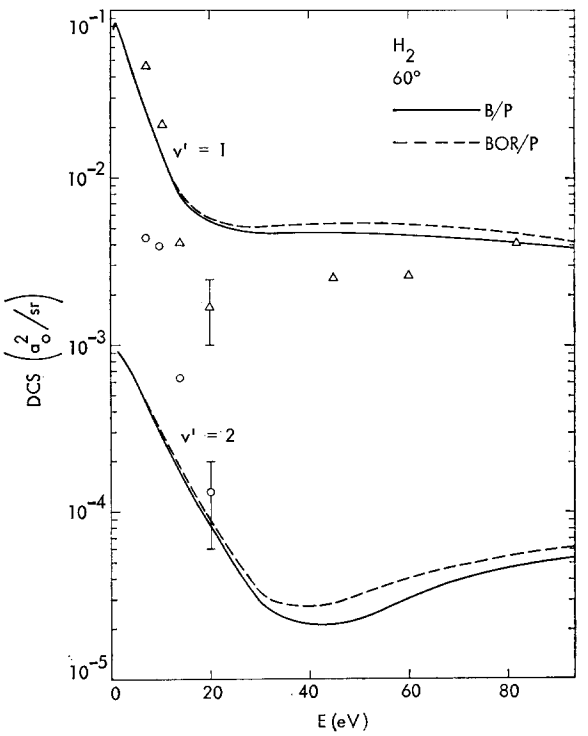

FIG. 31. Same as Fig. 29, except $\theta=60°$.

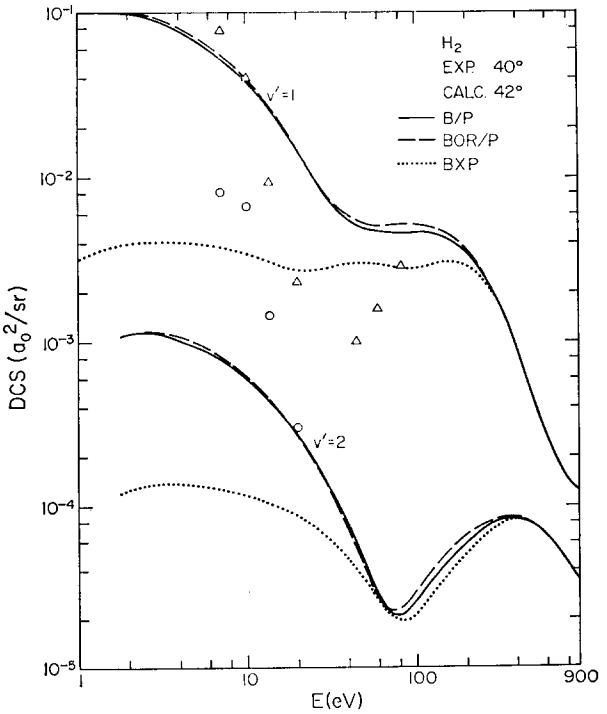

FIG. 30. The energy dependence of the DCS for vibrational excitation. The △ and the ○ are the present experimental results at $\theta=40°$ for $v'=1$ and $v'=2$, respectively. The curves are the present calculations at $\theta=42°$.

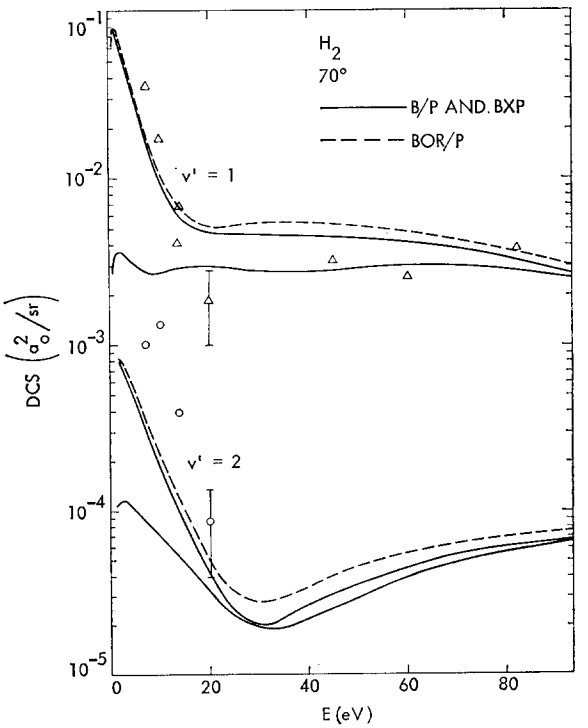

FIG. 32. Same as Fig. 29, except $\theta=70°$, and the results of the BXP calculation for DCS_{01} and DCS_{02} are also shown. The BXP cross sections are the lower solid curves.

D. Energy Dependence of the Differential Cross Sections

The energy dependencies of the present experimental and theoretical differential cross sections are shown explicitly in Figs. 28–34. Erhardt *et al.*[6] also measured the energy dependence (for $E \lesssim 10$ eV) of the differential cross section at 20°. We compare the two sets of results in Fig. 28; for the comparison we normalize Erhardt's data such that his DCS_{01} (20°) is equal to ours at $E=10$ eV. The agreement of the different experiments is seen to be good.

These figures show explicitly what follows from the comparison of the calculated and experimental elastic cross sections and scattering intensity ratios, e.g., that for the first vibrational excitation the calculated- and experimental-cross-section-versus-energy curves differ considerably at low angles, but the agreement is good at high angles. For the overtone vibration, the angle-analyzed excitation functions seem to be very similar to the ones corresponding to the fundamental vibration. The experimental data are, however, limited to low energies for the overtone.

It is noteworthy that the experimental DCS_{01} is an increasing function of energy at energies near 60 eV. This behavior is especially striking in the 30°–60° range. While this behavior is not predicted quantitatively by the calculations, the BXP cross section, which peaks very close to threshold, is again an increasing function of energy at least one higher energy range at any angle. The B/P calculations also show minima, but they are smaller. The minima in the experimental DCS_{01} as functions of energy move to lower energies at higher angles. The BXP calculations are in approximate qualitative agreement with this trend at higher energies, but the present calculations do not predict this feature accurately.

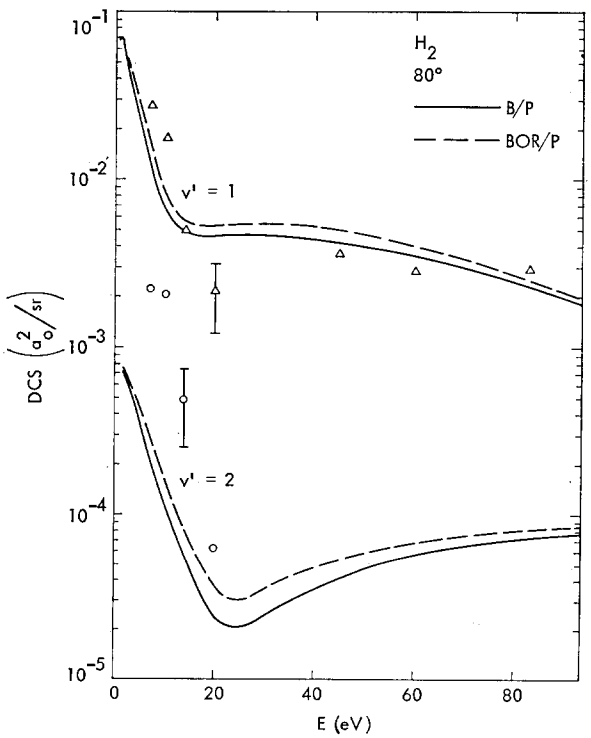

FIG. 33. Same as Fig. 29, except $\theta=80°$.

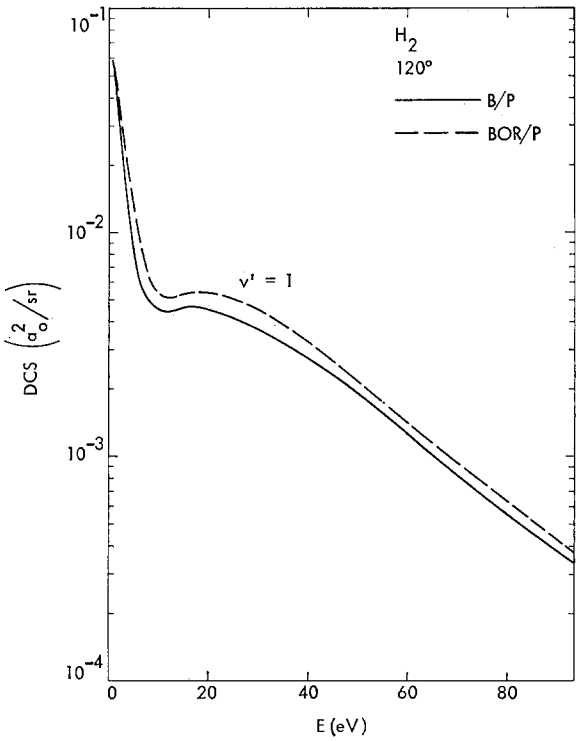

FIG. 34. The energy dependence of the DCS at $\theta=120°$ for excitation of the fundamental vibration as calculated in the polarized B/P and BOR/P approximations. The inclusion of polarization in the calculation makes less than 18% difference above 35 eV.

E. Energy Dependence of the Integral Cross Sections

The excitation functions $Q_{01}(E)$, $Q_{02}(E)$, and $Q_{03}(E)$ are shown on Figs. 35–36.

The experimental values of Ramien[1] and Ehrhardt *et al.*[6] are in good agreement with our measurements. Ramien's data are from multiple-scattering experiments in which he obtains the ratio of the number of inelastic collisions (with energy loss 0.5 eV) to the total number of collisions, i.e., approximately $Q_{01}/Q_{(00}+Q_{01})$. From this ratio, we obtained and plotted Q_{01} by using the cross sections of Golden, Bandel, and Salerno.[22] The difference between the results of Ehrhardt *et al.* and our data are within the combined errors of the experiments and the extrapolations of the DCS's to 180°. The B/P and BOR/P calculations yield Q_{01}'s which agree within a factor of 3 with experiment over the 1.5–100-eV energy range.

For the overtone vibrational excitations, the two sets of experimental integral cross sections are in agreement within their error limits. The calculated

TABLE II. Calculated integral vibrational excitation cross sections ($10^{-5}a_0^2$) for $v'=3$.

E (eV)	10	20	45	60	81.63	100	500
B/P	12.9	6.6	4.3	4.7	5.3	5.5	2.1
BOR/P	15.9	7.3	4.7	5.0	5.6	5.8	
BXP	6.1	3.3	2.8	3.6	4.5	4.8	2.0
BORXP	8.9	4.0	3.2	3.9	4.7	5.1	

cross sections are also in agreement with experiment at 20 and 40 eV; at the lower energies, however, they are about an order of magnitude smaller than the experimental values. This discrepancy is discussed at the end of this section.

Note added in proof: A new experimental study [A. Weingartshofer, H. Ehrhardt, V. Hermann, and F. Linder (to be published)] yields values for the "potential scattering" DCS's (in atomic units) in the 10.8–12.6 eV impact energy range at $\Theta=10°$ of 0.065, 0.0046, and 0.0006 for $v'=1$, 2, and 3, respectively. These cross sections do not include the scattering due to the 11–13 eV resonances but do include the tail of the 3 eV $^2\Sigma_u^+$ resonance discussed above. We can obtain the comparable experimental quantity by interpolating our results at 10 and 13.6 eV. This yields 0.08 and 0.009 for DCS_{01} and DCS_{02}, respectively. The calculations in the polarized Born and polarized Born–Ochkur–Rudge approximations yield 0.13, 0.002, and 0.00006 for the DCS's for $v'=1$, 2, and 3, respectively. The conclusions are similar to those we draw from our own experimental results at 10 eV.

Since there is very little information available for the excitation of the second overtone, our calculated integral cross sections for this process are given in Table II. The BOR/P calculation is the most reliable estimate of these cross sections presently available.

It has long been known that the static potential alone cannot account for the order of magnitude of the vibrational excitation cross sections at low energies. Figure 35 shows the calculated cross sections for vibrational excitation ($v'=1$) due to scattering off the static potential ($S_0S_2Q_2^{B'}$) and off the spherically symmetric component of this potential (S_0). Our experimental and theoretical results show that the static potential becomes so much more important at higher energies that it cannot be neglected even for qualitative work above 20 eV. Breig and Lin did plane wave calculations below 10 eV using only the spherically sym-

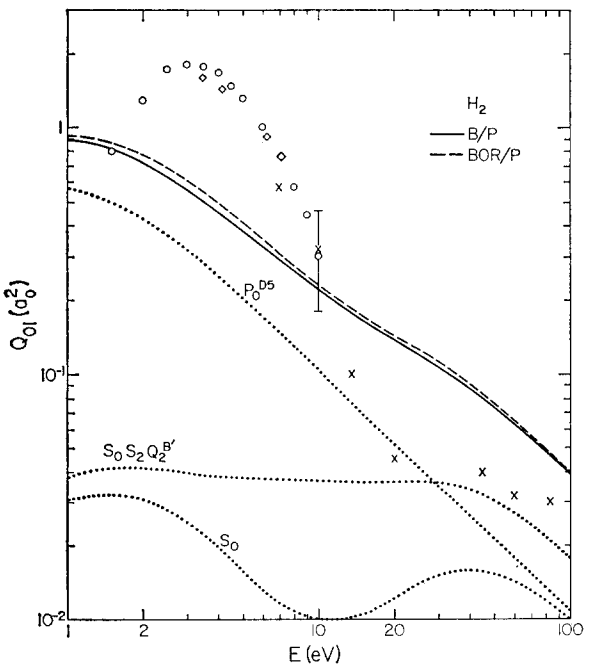

FIG. 35. Integral cross sections for the excitation of the fundamental vibrations ($v'=1$) as a function of impact energy. The symbols ×, ○, and ◇ represent the results of this paper, of Ehrhardt *et al.*, and of Ramien, respectively. The curves are the present calculations using data set 1. The dotted curves are calculated using only the amplitudes indicated (in the notation of Paper I).

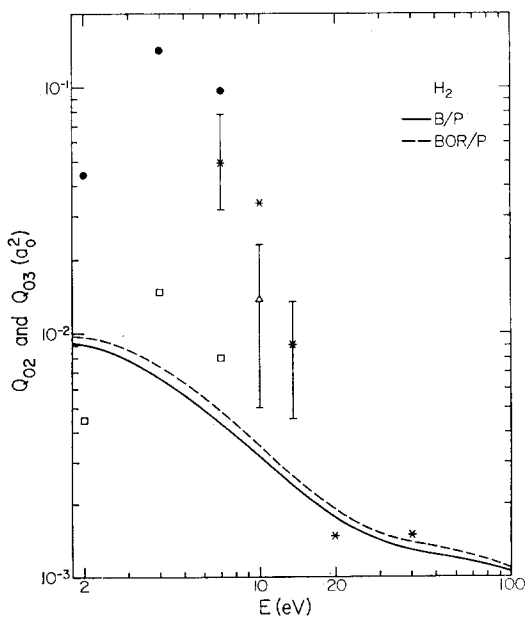

FIG. 36. Integral cross sections for the excitation of the first two overtone vibrations ($v'=2$ and 3) as a function of impact energy. Experimental cross sections are obtained from Ehrhardt *et al.* (● for $v'=2$, □ for $v'=3$) and from the present measurements (* for $v'=2$, △ for $v'=3$). Typical error bars are shown on some of our results. Theoretical cross sections are shown only for $v'=2$ because the theoretical curves for $v'=3$ are too small to fit on scale.

metric part of the polarization potential for the scattering.[16] They showed that this calculation could predict scattering of the correct order of magnitude. In Fig. 35 we show a calculation which uses only our DS1 polarization potential. Breig and Lin showed that it is possible using just the polarization potential to get more quantitative agreement with experiment at low energies by empirically increasing the potential's depth. This led to a $D8$ polarization potential with $a_p=1.3a_0$ (using the notation of Paper I). Such a potential has a depth of 0.604 hartree[23] at $r=1.34a_0$. This potential appears unrealistic because the Lane–Henry polarization potential (see Paper I and Ref. 19) has a maximum depth of 0.095 hartree at $r=1.50a_0$, while the deeper static potential is deepest at $r=0.70a_0$. Breig and Lin's incomplete procedure also leads to the prediction of qualitatively incorrect DCS's (see Paper I). Takayanagi did distorted wave calculations for the spherically symmetric part of the polarization potential.[17] His calculations, like Breig and Lin's were exploratory and cannot be used for quantitative estimation of cross sections because he used an oversimplified potential and unrealistic values for the cutoff radius. Nevertheless, his calculations do show that the distorted wave and plane wave treatments agree fairly well at low energies when compared for similar potentials and values of the cutoff radius.

Ehrhardt *et al.*[6] showed that at very low energies the vibrational excitation cross sections can be qualitatively explained using resonance theory. The resonance can be seen, for example, on Fig. 35. This resonance is a shape resonance in the $p\sigma$ partial wave and is associated with the $^2\Sigma_u^+$ state of H_2^- ions.[24] Our discussion of the 7–10-eV differential cross sections, however, has shown that potential scattering can account at least approximately for the $v'=1$ excitation cross section. It is interesting therefore to attempt a crude breakdown of the low-energy scattering into resonance and potential scattering contributions. Bardsley[25] showed that the integral cross section curve $Q_{ml,pp'}^{\rm res}$ for excitation of state p' $(=v'J'M')$ of the electronic ground state g from state p $(=vJM)$ of the same electronic state by means of temporary formation of the vibrational states n of the intermediate electronic state (resonance state) d having $l=1$, $m=0$ $(^2\Sigma_u^+)$ is given by

$$Q_{01,pp'}^{\rm res}=(4\pi/k_pk_{p'})\,|\sum_n f_{p'n}^{gd}f_{pn}^{gd}(\epsilon_n+i)^{-1}\,|^2, \qquad (6)$$

where l and m refer to the orbital angular momentum of the scattering electron and to the component of this angular momentum along the internuclear axis, respectively. The f's are the Franck–Condon factors, k_p and $k_{p'}$ are the wavenumbers of the incident and scattered electron,

$$\epsilon_n=(E-E_n)/\tfrac{1}{2}\Gamma, \qquad (7)$$

E is the impact energy, E_n is the energy of the resonance state with respect to the ground state of H_2 and a separated electron, and Γ is the width of the resonance. Bardsley *et al.*[7] have estimated theoretically that $\frac{1}{2}\Gamma=4.5$ eV, but we will use the value $\frac{1}{2}\Gamma=3$ eV estimated by Ehrhardt *et al.*[6] from their experiments. If we assume that the rotational state doesn't change and that only one vibrational state r of the resonance contributes, we can rewrite (6) as

$$Q_{01,vv'}^{\rm res}=A(v,v',r)/k_vk_{v'}(\epsilon_r^2+1), \qquad (8)$$

where the numerator A is independent of impact energy. Finally, without making a partial wave decomposition of the potential scattering cross section $Q_{vv'}^{\rm pot}$, the simplest approximation we can use for the full (resonance+potential scattering) integral cross section is

$$Q_{vv'}=Q_{vv'}^{\rm res}+Q_{vv'}^{\rm pot}. \qquad (9)$$

This amounts to neglecting terms due to interference of the resonance and potential scattering in the $l=1$ partial wave. We will further make the approximation that $Q_{vv'}^{\rm pot}$ can be estimated from our B/P calculations (with data set 1).

For this one state resonance model, we estimate from the cross sections of Ehrhardt *et al.*[6] that $E_r=3.5$ eV. Using Eq. (9), we also obtain from their data estimates of $Q_{01,0v'}^{\rm res}$ at $E=3.5$ eV. Then we use Eqs. (7) and (8) to calculate empirical values for $A(0,v',r)$ for $v'=1$, 2, and 3.

Next, Eq. (8) with the value of A determined above is used to predict $Q_{01,0v'}^{\rm res}$, at energies above 3.5 eV. Finally, the model's predictions for the full $Q_{0v'}$ are calculated from Eq. (9), and these cross sections are compated with experiment in Table III. In view of the approximations involved, these results can be considered only as qualitative estimates of the true situation. For the $v'=1$ case this crude model gives good agreement with experiments up to 10 eV and indicates that above about 7 eV the contribution from potential scattering is comparable to or larger than the one from resonance scattering.

For the excitation $v=0\rightarrow v'=1$, a more realistic model would include at least the $r=0$ and $r=1$ vibrational states of the resonance. The disagreement of the model and experiment for the energy dependence of Q_{01} would be lessened for a two vibrational-state resonance model because the added resonance state would raise the cross section more at 5 eV than at 10 eV. Ehrhardt *et al.*[6] interpreted the unsymmetrical shape of the Q_{01} curve as meaning that several states of the negative ion are important. It seems more probable, however, that only the lowest $(v'+1)$ states are very important and that the rest of the tail in the Q_{01} curve is due to contributions from potential scattering. For the higher v', the agreement between the predictions of this model and the experiments become progressively worse. The table indicates that excitation of these states is much closer to being pure resonance scattering than is the $v'=1$ excitation. The one-state model predicts that the cross

TABLE III. Summary of estimated resonance and potential scattering contributions to the integral cross sections (a_0^2).

		Calculation			Experiment	
v'	E (eV)	Res.	Pot.[a]	Sum.	ELLT[b]	TTRK[c]
1	3.5	1.256[d]	0.504	1.760[e]	1.76	
1	5	0.699[f]	0.380	1.079[g]	1.32	...
1	7	0.260[f]	0.290	0.550[g]	0.80	0.57
1	10	0.075[f]	0.221	0.296[g]	0.31	0.32
2	3.5	0.13[d]	0.007	0.137[e]	0.14	
2	5	0.069[f]	0.006	0.075[g]	0.12	...
2	7	0.025[f]	0.004	0.029[g]	0.096	0.050
2	10	0.007[f]	0.003	0.010[g]	...	0.034
3	3.5	0.015[d]	0.0002	0.0152[e]	0.015	
3	5	0.0055[f]	0.0002	0.0057[g]	0.012	...
3	7	0.0025[f]	0.0002	0.0027[g]	0.008	...
3	10	0.0005[f]	0.0001	0.0006[g]	...	(0.014)

[a] Present B/P calculation (DS1).
[b] Reference 5.
[c] Present results.
[d] Taken as Column 5 minus Column 4.
[e] Taken as equal to Column 6.
[f] Calculated from Eq. (8).
[g] Taken as sum of Columns 3 and 4.

sections decrease too rapidly with energy. Since we probably have not underestimated the potential scattering (the comparison of theory and experiment in the nonresonant regions indicates that our theoretical treatment overestimates the potential scattering cross section), this error is probably due to our oversimplified treatment of the resonance. One defect of the model is that the $n=2$ and 3 states, which it neglects, probably are more important for excitation of these higher vibrational states. Also, perhaps the results indicate that a half-width larger than 3 eV should be used. Both these corrections would raise the predicted cross sections at energies above 3.5 eV.

V. CONCLUSIONS

The differential cross sections for vibrational excitation of $v'=1$ level of H_2 are strongly decreasing functions of scattering angle in the 10°–30° region for $E=7$–81.6 eV. At energies above 20 eV they show a deep minimum near 30°. The polarized Born and polarized prior Born–Ochkur–Rudge calculations are in qualitative agreement with experiment except that they do not give a deep enough minimum in the differential cross section. The energy and angle dependence of the quantum-mechanical cross sections is quantitatively very good in the 50°–80° range. For the integral cross sections, theory and experiment agree only within a factor of about 3, and the calculations seem to overestimate the nonresonance contributions to the cross sections in the intermediate energy range.

While Taylor and co-workers[6,9] interpreted the excitation of the $v'=1$, 2, and 3 levels at 10-eV impact energy as due mainly to resonance contributions, we find that the potential scattering (or direct interaction) contributions to the $v'=1$ excitation cross section are appreciable at 10 eV. However, these contributions decrease more rapidly with increasing v' than do those predicted by a resonance mechanism, so that excitation of the $v'\geq 2$ levels is evidently due primarily to resonance scattering even at 10 eV (about 7 eV away from the nominal resonance energy) (It has been shown for a long time that resonance scattering often leads to appreciable cross sections for processes with large Δv.[26]) However, at higher energies ($E=20$–45 eV) our first-order calculations account quantitatively for the magnitude of the $v'=2$ cross sections. Both experimentally and theoretically, the shapes of the differential cross sections for exciting the $v'=1$ and the $v'=2$ levels are similar to each other as compared to the shapes of the DCS's for elastic scattering[14] or excitation of the $b\,^3\Sigma_u^+$ or the $a\,^3\Sigma_g^+$ states.[27]

ACKNOWLEDGMENT

We wish to thank Dr. R. T. Brinkmann for his help in processing the experimental data.

* Jet Propulsion Laboratory. Work supported in part by the National Aeronautics and Space Administration under Contract No. NAS7-100.
† A. A. Noyes Laboratory of Chemical Physics, Contribution No. 3965. Work supported in part by the U.S. Atomic Energy Commission under Report Code CALT-767P4-56.
‡ Present address: Division 5232, Sandia Laboratories, Sandia Corporation, Albuquerque, N.M. 87115.

[1] H. Ramien, Z. Physik **70,** 353 (1931).
[2] V. A. Bailey, Phil. Mag. **13,** 993 (1932).
[3] A. G. Engelhardt and A. G. Phelps, Phys. Rev. **131,** 2115 (1963); A. V. Phelps, Rev. Mod. Phys. **40,** 399 (1968).
[4] G. J. Schulz, Phys. Rev. **135,** A988 (1964).
[5] M. G. Menendez and H. K. Holt, J. Chem. Phys. **45,** 2743 (1966).
[6] H. Ehrhardt, L. Langhans, F. Linder, and H. S. Taylor, Phys. Rev. **173,** 222 (1968).
[7] J. N. Bardsley, A. Herzenberg, and F. Mandl, Proc. Phys. Soc. (London) **79,** 305, 321 (1966).
[8] J. N. Bardsley and F. Mandl, Rept. Progr. Phys. **31,** 471 (1968).

[9] T. F. O'Malley and H. S. Taylor, Phys. Rev. **176,** 207 (1968).
[10] F. H. Read, J. Phys. B **1,** 893 (1968); J. N. Bardsley and F. H. Read, Chem. Phys. Letters **2,** 333 (1968).
[11] H. S. Taylor, "Models, Interpretations and Calculations Concerning Resonant Electron Scattering Processes in Atoms and Molecules," Advan. Chem. Phys. (to be published).
[12] J. Comer, F. R. Read, International Conference on the Physics of Electronic and Atomic Collisions 6th, 1969, 86 (1969), Abstracts; A. Weingartshofer, H. Ehrhardt, and F. Linder, *ibid.*, p. 91.
[13] J. Geiger and K. Wittmaack, Z. Physik **187,** 433 (1965).
[14] S. Trajmar, D. G. Truhlar, and J. K. Rice, J. Chem. Phys. **52,** 4502 (1970), preceding article, Paper II.
[15] D. G. Truhlar and J. K. Rice, J. Chem. Phys. **52,** 4480 (1970). This article will be referred to as I.
[16] E. L. Breig and C. C. Lin, J. Chem. Phys. **43,** 3839 (1965).
[17] K. Takayanagi, J. Phys. Soc. Japan **20,** 562 (1965).
[18] T. R. Carson, Proc. Phys. Soc. (London) **A67,** 909 (1954).
[19] N. F. Lane and R. J. W. Henry, Phys. Rev. **173,** 183 (1968).
[20] D. G. Truhlar, J. K. Rice, A. Kuppermann, S. Trajmar, and D. C. Cartwright, Phys. Rev. (to be published).
[21] C. Ramsauer and R. Kollath, Ann. Physik **4,** 91 (1929); **12,** 529 (1932).
[22] D. E. Golden, H. W. Bandel, and J. A. Salerno, Phys. Rev. **146,** 40 (1966).
[23] 1 hartree = 27.210 eV = 4.3592×10^{-11} erg.
[24] H. S. Taylor, G. V. Nazaroff, and A. Golebiewski, J. Chem. Phys. **45,** 2872 (1966).
[25] J. N. Bardsley, Chem. Phys. Letters **2,** 329 (1968).
[26] G. J. Schulz, Phys. Rev. **125,** 229 (1962).
[27] S. Trajmar, D. C. Cartwright, J. K. Rice, R. T. Brinkmann, and A. Kuppermann, J. Chem. Phys. **49,** 5464 (1968).

THE JOURNAL OF CHEMICAL PHYSICS VOLUME 52, NUMBER 9 1 MAY 1970

Plasma Effects in Annulene Molecules

DAVID B. CHANG
Boeing Scientific Research Laboratories and University of Washington
AND
JAMES E. DRUMMOND
Boeing Scientific Research Laboratories, Seattle, Washington 98124

(Received 20 October 1969)

Some plasma effects of the pi electrons in annulene molecules are studied. The dispersion relation for plasma oscillations, obtained by using Hückel molecular orbitals in the second quantization formalism, is found to describe soundlike waves. The resulting polarization response of the pi electrons causes a spatial modulation of the interaction potential between two pi electrons. The polarization response defines the natural correlation units in annulenes to be quartets in all but the angular momentum $l=\pm 2n$ states of $4n$-annulenes and zero angular momentum states, where the correlation unit is a pair of electrons. Correlation is discussed by using the modified interaction potential with a Wannier hamiltonian in pair and quartet equations. The effect of band alternation is considered in connection with the variation of induced currents in unsaturated annulenes with temperature.

I. INTRODUCTION

In this paper we study some plasma effects of the pi electrons in annulene molecules. We consider first the form that the plasma oscillations take in these cyclic polyenes, and then discuss polarization and correlation consequences. In Sec. II the dispersion relation for plasma oscillations is derived by using Hückel molecular orbitals as the single-particle eigenfunctions in the second quantization formalism. In Sec. III the resulting polarization response of the pi electrons is obtained, and the modification of the interaction potential between two pi electrons is described. Correlation is discussed in Sec. IV by using the modified interaction potential with a Wannier Hamiltonian in pair and quartet equations. The plasma effects are summarized and discussed in Sec. V.

II. DISPERSION RELATION

The dispersion relation for plasma oscillations may be obtained by combining Schrödinger's equation with Poisson's equation in the self-consistent field approximation.[1,2] Denoting the wavefunction of the N pi electrons in N-annulene by $|\ \rangle$ and their Hamiltonian by $H=H_0+H_1$, we have

$$ih(\partial/\partial t)\,|\ \rangle=(H_0+H_1)\,|\ \rangle. \tag{1}$$

Here, H_0 denotes the sum of the kinetic energy of the pi electrons and potential energy of the pi electrons in the periodic potential formed by the ion cores and the electrons in their ground state. The details of H_0 will be discussed further in connection with correlation in Sec. IV. H_1 denotes the potential energy of the pi electrons in a potential $\Phi(\mathbf{r}, t)$, where $\mathbf{r}$ is the position vector and t is the time. In the second quantization formalism, H_0 and H_1 may be expressed in terms of the creation and annihilation operators $c_n^\dagger$ and c_n for the single-particle molecular orbital eigenfunctions ψ_n given by H_0 as

$$H_0=\sum_n c_n^\dagger c_n E_n, \tag{2}$$

$$H_1=-e\sum_{m,n}\langle m\,||\,\Phi\,||\,n\rangle c_m^\dagger c_n. \tag{3}$$

In these expressions, E_n is the eigenvalue corresponding to ψ_n, $-e$ is the electronic charge, and

$$\langle m\,||\,\Phi\,||\,n\rangle\equiv\int\psi_m^*(\mathbf{r}')\Phi(\mathbf{r}', t)\psi_n(\mathbf{r}')\,d\mathbf{r}^{3\prime}, \tag{4}$$